Excerpt from the Proceedings of the 2011 COMSOL Conference in Boston

Carbon MEMS Accelerometer

Jennifer Strong*[1], Cody M. Washburn[2], Randy Williams[2], John McBrayer[2], Tedd Rohwer[2], Regan Stinnett[2], Patrick Finnegan[1], Brad Hance[2], Doug Greth[2], and Dave R. Wheeler[2]
[1]LMATA Government Services, LLC, Albuquerque, NM 87109
[2]Sandia National Laboratories, Albuquerque, NM 87185
*Corresponding author: Sandia National Laboratories, Albuquerque, NM 87185, jmstron@sandia.gov

Abstract: The newly emerging field of carbon-based MEMS (C-MEMS) attempts to utilize the diverse properties of carbon to push the performance of MEMS devices beyond what is currently achievable. Our design employs a carbon-carbon composite using nano-materials to build a new class of MEMS accelerometer that is hyper-sensitive over a dynamic range from micro-G to hundreds of G's – far surpassing the capabilities of currently available commercial MEMS accelerometers.
Validating single cantilever beams of a 10:1 aspect ratio has shown only a 2% error from predicted to actual deflection calculations, while a clamped-clamped U-beam with 5% multi-walled carbon nanotubes describes a nearly 30% increase in Young's modulus and begins demonstrating tunable material properties through nano-material loading in MEMS devices.

Keywords: carbon MEMS, C-MEMS, carbon-carbon composites, accelerometer

1. Introduction

A carbon-carbon composite MEMS accelerometer, using nano-material stiffeners, drives new materials and devices into micro-electro mechanical systems to improve dynamic range, sensitivity, lifetime, and functionality when compared to state of the art MEMS technology. The proposed carbon composite structure is a replacement for single crystal/metal MEMS beams, flexures, struts etc. at a fraction of the expense. These materials are less prone to stiction under high G-force loading, and have tremendous resilience under extreme mechanical deformation and shock.
The pyrolysis of photo-patternable materials has been described by George Whitesides, et. al. [1], which describes the basic micro-electromechanical properties related to pyrolytic carbon materials and resonator devices using a 15 GigaPascal (GPa) Young's Modulus. Since then, Marc J. Madou, et. al.[2] U.C. Irvine and Richard L. Mcreery, et. al.[3] University of Alberta, CA have developed carbon on carbon approaches to develop carbon micro-electromechanical systems, high surface area electrochemical sensors, along with carbon for anode/cathode materials for Li-ion battery applications. Groups at Sandia have demonstrated pyrolytic carbon's remarkable abilities by electrochemically placing nano-materials on the surface for bio-applications [4].

The MEMS single beam, clamped-clamped U-beam and diaphragm carbon-carbon composite structures provide the basis of testing and evaluating nano-materials in patterned carbon matrices. Nano-material loading into various polymer precursors and carbon matrices has been shown [5,6] to directly impact spring constant and Young's modulus of the final material. Modeling and validating nano-material structures is a new challenge to finite elemental analysis (FEA) and this is an initial attempt to start merging data collected with modeling efforts.

2. Device Fabrication

Devices are fabricated using a 4 inch silicon 1-100 ohm-cm wafer, which are cleaned using acetone, methanol and isopropanol and dried with N2. Hexamethyldisilazane (HMDS), an adhesion promoter and dehydration bake prime the wafers for photolithography in an HMDS oven. The vapor primed wafers are spin coated to a thickness of 3.3 μm with photoresist from Clariant Chemical - AZ4330. Using a manual contact aligner, Karl Suss MA6, the wafers are exposed to 120 mJ/cm^2 of 365 nm light. The exposed resist is then developed using MF319 for approximately 125 seconds. A modified post exposure bake process is used by ramping a hotplate from 90 C, 10 C/min ramp, and holding at an elevated temperature of 280 C for 1 minute.

Pyrolysis to carbon is done under a high temperature reducing atmosphere producing a mechanical structure which is electrically active. A 3 C/ min. ramp rate is used with a Lindberg 3" tube furnace and a CoorsTek alumina tube of 5% hydrogen and 95% nitrogen atmosphere at 500 sccm flow. The program holds at 1100 C for 1 hour before passively cooling to room temperature. At this point the devices are

released from the silicon substrate by using a xenon difluoride etch process of 105 cycles to undercut the silicon away from the carbon by 85-90 μm.

Single cantilever beams, clamped-clamped U-beams and a diaphragm with a large proof mass were designed and fabricated using this approach, and are shown in Figure 1(a-c).

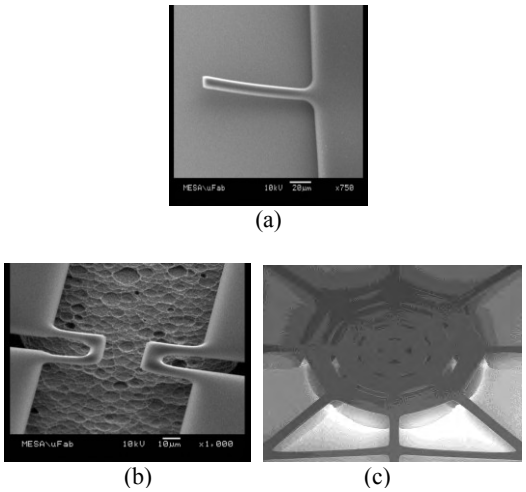

(a) (b) (c)

Figure 1. The (a) single cantilever beam, (b) clamped-clamped U-beam, and (c) proof mass diaphragm carbon MEMS device.

2.1 Multiwalled Carbon Nanotube Blending

Multiwalled carbon nanotubes (MWCNT) were purchased from Nanostructured and Amorphous Materials Inc., with a distribution of 40-70 nm in diameter and 0.5 μm to 5.0 μm in length and blended at 1%, 5%, 7% and 10% weight percent into Clariant chemical AZ4330 photoresist. The same resist process was used, which included a 2 hour sonication step before spin coating to help minimize agglomeration of the nanotubes. Pyrolysis is necessary before etching as to allow the stress of the material to be conformal with the starting silicon substrate. The same xenon difluoride etch parameters were used to develop the clamped-clamped U-beam design, which is shown in Figure 2(a-d).

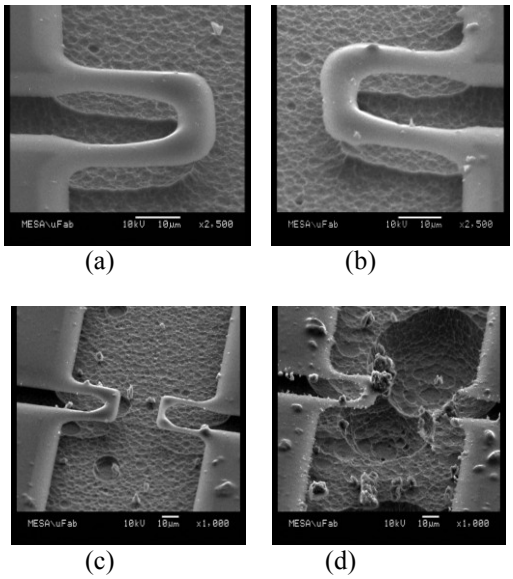

(a) (b) (c) (d)

Figure 2. SEMS of (a) 1%, (b) 5 %, (c) 7%, and (d) 10% clamped-clamped U-beam designs after etch release.

2.2 Device Dimensions and AFM Testing

During processing of the devices, the photo-active polymer passes through the glass transition temperature (Tg) approximately at 180 C before hardening to Bakelite. At this stage the lithographic mask dimensions and the final carbon device dimensions are biased due to the reflow of the photoresist. Table 1 describes the device investigated and the final geometry of the unloaded (no tubes) carbon MEMS device tested under AFM.

Table 1. Lithographic Definition.

	Mask		Device		
Device	L (μm)	W (μm)	L (μm)	W (μm)	Thickness (μm)
Single Beam	100	10	106	11.6	1.0
U-Beam(w)	30	10	27	8.5	0.8
U-Beam(s)	30	7.5	27	6.0	0.8

The offset of the final device dimensions from the on mask dimensions are consistent on a single wafer.

A Veeco D5000 atomic force microscopy (AFM) tool was used to evaluate the devices in terms of force verse deflection measurements. Aluminum contact mode tips were purchased from Budget Sensors, model number: ContAl-G-10, with a resonant frequency of 13KHz (+/- 4KHz) and force constant of 0.2 N/m with a range of 0.07 to 0.4 N/m. Force versus distance data was collected using 1 V bias or 50 nano-Newtons (nN) of down force and a scan rate of 3.49 Hz using a 0.329 N/m tip. The above software and hardware configuration was used for all data collected.

3. COMSOL Multiphysics and Beam Theory

The use of COMSOL Multiphysics begins with a simple correlation of COMSOL geometry models to physical data. The purpose is two-fold: first, it allows a control on experiments by ensuring proper extraction of material properties from our test structure data. Second, it helps to ensure that modeling complex design geometries in COMSOL yields practical and usable data that allows MEMS designers to build meaningful predictions.

Nano-material composites in MEMS fabrication have material properties that are either non-existent or poorly characterized in present literature. Investigating stationary structural mechanics and Young's modulus (E) in particular in carbon-carbon composites is an initial effort to understand the mechanical fundamentals. COMSOL helps validate that the method used to distill Young's modulus from physical test structures is reasonable. After calculating Young's modulus from test structure data using beam theory, that value of E is entered into the COMSOL model of that structure to make certain that the modeled deflection in COMSOL is reasonably close to the deflection expected from AFM force versus deflection curves.

The next steps involve correlating test data for more complex structures to their corresponding COMSOL models. Good correlation gives confidence that the COMSOL models accurately represent the physical structures and can be used to guide design. A poor correlation yields useful information as well, pointing to either a disparity between the COMSOL model and the physical structure, or to a misunderstanding of the physical structures or materials due to fabrication errors which are coupled with complex nano-material interactions.

Following a successful correlation of the complex physical structures to corresponding models in COMSOL, the models will guide design optimization by enabling us to parametrically sweep through a wide range of key dimensions for each design and fine-tune the design for the desired responses. Using COMSOL for the design optimization phase will considerably shorten both the time required and the materials consumed for optimization by eliminating the necessity of fabricating and testing numerous structures with small design variations.

3.1 Cantilever Beam Theory

The test structures pictured in Figure 1(a) are essentially simple cantilevered beams, and can be approximated as a linear beam of rectangular cross section with one fixed end and one free end. The force load (F) is applied to the free end of the beam. The beam has a given length (L), width (b), and thickness (h). Equation 1 gives the theoretical maximum deflection (δ) of such a beam, where E is Young's modulus and I is the second moment of inertia.

$$\delta = \frac{FL^3}{3EI} \qquad [1]$$

For a beam with a rectangular cross section, I can be calculated using Equation 2.

$$I_x = \frac{bh^3}{12} \qquad [2]$$

Using the expression for I given by Equation 2, Equation 1 can be re-written as Equation 3.

$$\delta = \frac{4FL^3}{bh^3E} \qquad [3]$$

In this case, the value of E is an unknown. However, AFM data provides basic measurements of beam deflection under a given force, offering some insight into the elastic behavior of the beam. For now, it is assumed

that the force versus deflection is linear over the measurement range and follows the basic elastic relationship given by Equation 4, where k represents the theoretical spring constant of the cantilever beam in N/m.

$$k = \frac{F}{\delta} \qquad [4]$$

After using Equation 4 to calculate an average theoretical spring constant (k) for a specific cantilever structure using the AFM data, Equation 5 determines the theoretical deflection (δ) of the beam for a given value of F.

$$\delta = \frac{F}{k} \qquad [5]$$

Now that the theoretical deflection (δ) for a given force (F) is known, Equation 3 can be re-arranged:

$$E = \frac{4FL^3}{bh^3\delta} \qquad [6]$$

Equation 6 can now be used to calculate a value for Young's modulus (E).

3.2 U-Beam Calculations

Test structures included U-shaped beams which are clamped on both ends with the center of the beam free to deflect (see Figure 1(b)). The AFM tip is centrally located with respect to the center of the free end of the beam and beam width.

When using these beams to calculate Young's modulus (E), the U-beam is treated as two single simple cantilevered beams with the applied force (F) evenly distributed between the two cantilevers. This allows E to be computed using Equation 6. The applied force for a single beam is assumed to be the force applied to the U-beam divided by 2.

COMSOL verified the validity of these assumptions. A U-beam made from aluminum was modeled in COMSOL with a point load applied to the free end of the beam along the beam's axis of symmetry. A range of point load values was then applied to the model, and the corresponding maximum deflections were recorded. Next, a single cantilever beam version of the U-beam was modeled (essentially one side of the U-beam minus the bent portion of the beam) with a point load applied to the free end of the beam Again, a range of point loads was applied to the model and the maximum deflections were recorded. For any given load applied to the U-beam, the maximum deflection was 6.21% more than that of the cantilever (with the loading applied to the cantilever divided by 2 to approximate the full load being distributed over two cantilevers).

3.3 Modeled Beams

All COMSOL models start with the mask dimensions and are adjusted to account for various differences between the dimensions on the mask and the final product. These differences are mentioned briefly in Section 2.2. Specifically the final length and width dimensions are adjusted, fillets are added to corners to approximate the reflow of photoresist, and an undercut is added at the edge of the bond pads to approximate the lateral material removal that happens during the etch process. These adjustments can vary from wafer to wafer as the fabrication process is still undergoing research and development. Examples of specific COMSOL models used for single cantilever and U-beam structures are shown in Figure 3.

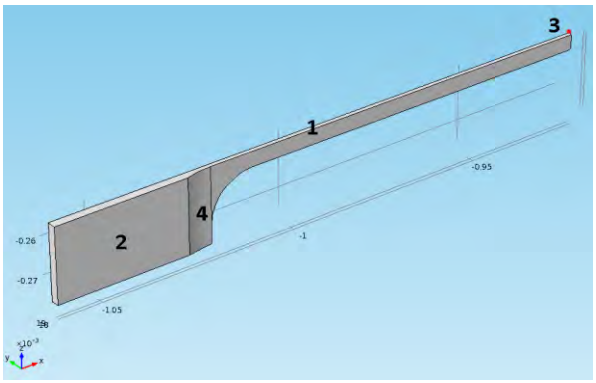

(a)

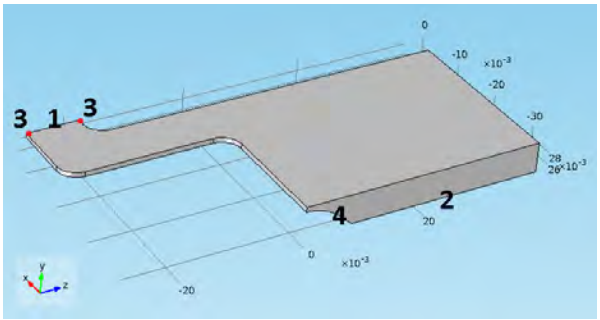

(b)

Figure 3. COMSOL models of the (a) single cantilever beam and (b) clamped-clamped U-beam. For both models, "1" represents the location of a symmetry boundary, "2" is the bottom of the bond pad which is a fixed surface, "3" represents the location of the point loads (which are applied in the –y direction), and "4" is the undercut area due to the etch. For the u-beam, the point load is first applied to the far end of the beam and the deflection is measured; then, the point load is applied to the part of the "u" that is closer to the fixed end and the deflection is measured again. These two deflections are averaged to get the final modeled deflection.

3.4 Modeled Diaphragm Structure

The diaphragm structure, pictured in Figure 1(c), is the design of most interest at this time. This design is currently being looked at from a strictly mechanical perspective, but ideally the modeling will eventually encompass all of the electromechanical properties that are of importance to the functioning of the final device. The COMSOL model of the diaphragm structure is shown in Figure 4.

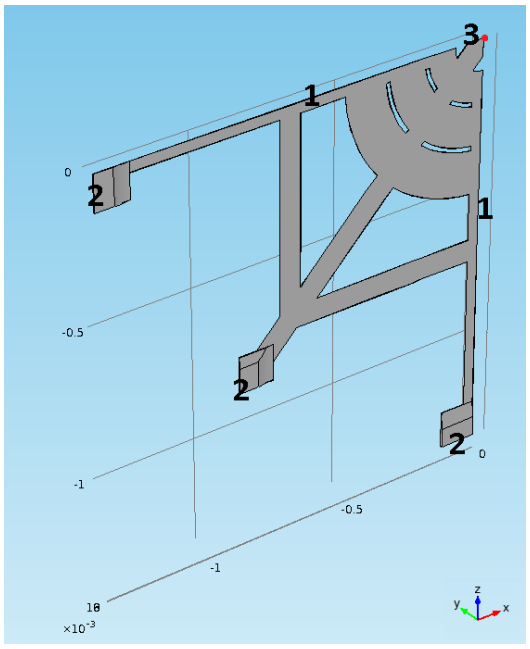

Figure 4. The COMSOL model of the diaphragm structure.

The labels "1," "2" and "3" hold the same meaning for Figure 4 as for Figure 3. The undercut area can be seen near the 3 fixed boundaries that represent the bond pads.

4. Data and Modeling Results

4.1 Single Cantilever Beam

Force versus deflection data was collected for a set of 10, 10μm cantilever beams made from 0% CNT loaded pyrolytic carbon. The theoretical spring constant was averaged for the 10 beams and subsequently used to extract a value for Young's modulus (E) for the material. The value obtained for E from this particular wafer was larger compared to earlier values of E obtained from U-beam structures on a different wafer (52.3 GPa versus 2.27 GPa). Standardization and tailoring of the fabrication process for a particular geometry should, together with more data, result in more consistent calculations of Young's modulus.

The COMSOL model correlated excellently for this particular cantilever structure. The predicted deflection was 403 nm for an applied force of 50nN while the modeled deflection was 411 nm, a difference of ~2%.

4.1 U-Beam Carbon-Carbon Composite

AFM data of U-beam structures loaded with MWCNTs at varying weight percent was gathered. Force versus deflection (δ) data for 4 beams, 2 wide U-beams and 2 skinny U-beams, was collected for each composite and used to calculate an average Young's modulus (E). Table 2 shows the calculated values of E for each composite.

Table 2. Young's Modulus vs. CNT Loading.

CNT Loading	Young's Modulus (GPa)
0%	2.22
1%	2.16
5%	3.01
7%	1.94
10%	2.16

The structures made from the 7 and 10% CNT loaded composites had fabrication issues due to the high loading of CNTs, as evidenced by the SEM images in Figure 2. This led to deflection measurements that are greater than expected, and consequently calculations for E that are likely inaccurate as compared to the calculations for the 0, 1%, and 5% CNT loaded composites.

Fabrication issues aside, the COMSOL U-beam models predicted deflection with low error for each given structure and given value of *E* with a chosen point load of 50nN. The percent difference between the modeled deflection and the deflection derived from the theoretical spring constant extracted from the AFM data is <5%, as shown in Table 3.

Table 3. Modeled Versus Predicted Deflections for the U-Beam Structures.

Beam Type	% CNT Load	Modeled δ (nm)	Predicted δ (nm)	% Difference
wide	0%	193	203	4.97%
wide	1%	199	209	4.97%
wide	5%	141	148	4.92%
wide	7%	222	233	4.80%
wide	10%	200	209	4.68%
skinny	0%	290	288	0.79%
skinny	1%	298	296	0.71%
skinny	5%	211	209	0.56%
skinny	7%	332	330	0.72%

4.3 Diaphragm Structure

While collecting force versus deflection data for the 0% CNT loaded pyrolytic carbon 10μm cantilever beams, data was also collected for a set of 8 diaphragm structures off of the same wafer. The averaged theoretical spring constant for all 8 structures was used to predict the deflection expected from the COMSOL model of the diaphragm.

The diaphragm structure has a predicted deflection of 238 nm for an applied force of 50nN. This does not correlate well to the deflection of 849 nm obtained from the COMSOL model. The reason for the poor correlation is still being investigated. The diaphragm structures on this particular wafer appeared to have a significant amount of internal stress. See Figure 5.

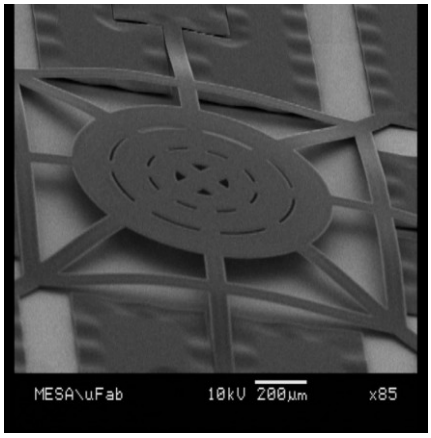

Figure 5. A recently fabricated diaphragm structure.

As illustrated in Figure 5, the diaphragm structure is bowed significantly out of plane. This could be affecting the force versus deflection measurements taken using the AFM, causing a poor correlation to the COMSOL model which is modeled as a flat, in-plane structure.

5. Conclusions

The development of a tunable material set using carbon nanotubes in an accelerometer is inconclusive, while the use of COMSOL modeling assisted in validating the 30% improvement in Young's modulus over pyrolytic carbon. The procedure to correlate and validate a finite element model is still being developed, with as low as 2% error being achieved from single cantilever beams with a 10:1 aspect ratio. Device processing, polymer reflow, and carbon nanotube blending and suspension have critical components which relate to the final carbon MEMS devices and more data is required to understand many of these challenges.

A diaphragm designed accelerometer with a central proof mass has multiple complex geometries and pushes mechanical understanding and modeling of these carbon-carbon composite structures and devices. COMSOL will be essential in shortening and optimizing the design and manufacturing feedback schedule for future device fabrication.

6. References

1. G.Whitesides, et. al. “Fabrication and Characterization of Glassy Carbon MEMS”, Chem. Mat. 1997, 9, 1399-1406
2. M. Madou, et. al. “Fabrication of suspended carbon microstructures by e-beam writer and pyrolysis”,2006, (13), 2602-2607
3. R. Mcreery, et. al. ” Photoresist-Derived Carbon for Microelectromechanical Systems and Electrochemical application” Journal of The Electrochemical Society, 147, (1) 277-282
4. Polsky, et. al.” Lithographically Defined Porous Carbon Electrodes”, vol. 5, (24), 2792-2796
5. T. Yamada, et. al.” A stretchable carbon nanotube strain sensor for human motion detection”, Nature NanoTech., 3/27/2011, DOI: 10.1038
6. T. Ramanathan, et. al. “Functionalized graphene sheets for polymer nanocomposites”, Nature NanoTech., 6/2008, vol.3, DOI: 10.1038

7. Acknowledgements

The authors would like to thank Dick Grant, Christine Ford, Jeff Stevens, NINE funding, and other sponsored support of this work. Sandia National Laboratories is a multi-program laboratory managed and operated by Sandia Corporation, a wholly owned subsidiary of Lockheed Martin Corporation, for the U.S. Department of Energy's National Nuclear Security Administration under contract DE-AC04-94AL85000.